VLA observations of a 5 arcsec radio galaxy at 4.9 GHz*

Qing Zhou†
(Dated: 1, December, 2017)

Active galactic nuclei (AGNs) are the most compact regions sitting in the centre of galaxies, emitting high energy radiation which contains information about the formation and evolution of galaxies. The emission is high in radio window, thus studying radio-loud AGNs are very essential to radio astronomy. In this paper, the properties of a radio galaxy 4C +00.35 were studied, based on the observation by the Very Large Array (VLA) on Jul 30, 1994. The total flux density were found to be (363.65±27.0)mJy and peak densities 112.3 mJy and 79.9 mJy respectively, each having an uncertainty of 27 mJy. The spectral index in the lower frequency range was -0.69; whereas the spectral index found in the higher frequency range was -3.74, which confirms it is a radio-loud galaxy.

Key words: Radio Sources, Galaxies: active, Galaxies: radio, AGN, Techniques: interferometric

I. INTRODUCTION

A. Radio Galaxies

Radio galaxies and their relatives, radio-loud quasars and blazars, are types of active galaxy that are very luminous at radio wavelengths, with luminosities up to 1039 W between 10 MHz and 100 GHz.[1] The emitting of high-energy relativistic jets are due to the synchrotron process caused by the high energy particles moving close to the speed of light in a compact magnetic field. The observed structure in radio emission is determined by the interaction between twin jets and the external medium, modified by the effects of relativistic beaming. The host galaxies are almost exclusively large elliptical galaxies. Radio-loud active galaxies can be sub-divided into two classes according to their emission mechanisms, namely low-excitation and high excitation classes. They can be detected at large distances, making them valuable tools for observational cosmology.

B. Active Galactic Nuclei

An active galactic nucleus (AGN) is the central region of a galaxy where in most cases the luminosity is at its peak. The spectrum of an AGN observed is unlike that of any other astrophysical object. The emission is found to be bright at all wavelengths. Besides, the luminosity of the central region varies on a very short timescale, less than a day, implying that the size of the central region is less than one light-day across[1]. This high luminosity in a small region (more than $2 \times 10^{10} L_{\odot}$[2] produced within a tiny volume) yields a high conversion of matter into energy, resulting in the accretion around a supermassive black hole, one of the most compact objects in the universe. Most ($\sim 90\%$) of AGNs are radio quiet and some are also obscured by gas and dust, making large amount of radio emission hard to be detected directly. Thus studying radio-loud active galaxies is essential to understanding the kinematics and dynamics of AGNs.

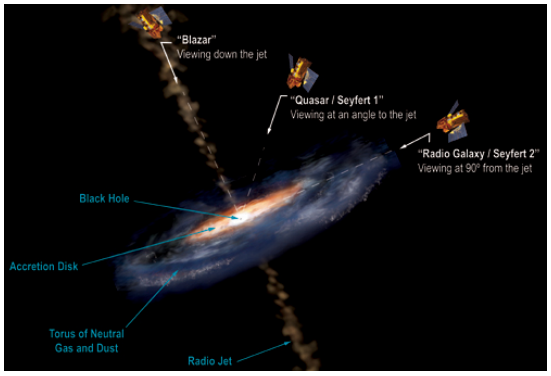

FIG. 1. Illustration of an AGN: This illustration shows the different features of an active galactic nucleus (AGN), and how our viewing angle determines what type of AGN we observe. The extreme luminosity of an AGN is powered by a supermassive black hole at the center[3]. Image credit: Aurore Simonnet, Sonoma State University.

Fig.1 shows how different viewing points are related to varying types of AGNs. The extreme luminosity of an AGN is powered by a super-massive black hole in the centre. When viewed from 90°, the high-energy relativistic jets from radio-loud galaxies can be detected in the radio window.

C. Very Large Array

The Karl G. Jansky Very Large Array (VLA) is a centimeter-wavelength radio astronomy observatory located in central New Mexico on the Plains of San Agustin, between the towns of Magdalena and Datil, $\sim$ 50 miles (80 km) west of Socorro. The VLA consists of twenty-seven 25-meter radio telescopes deployed in a Y-shaped array and all the equipment, instrumentation, and computing power to function as an interferometer.

---

* 3^{rd} report of Introduction to Radio Astronomy

† Kapteyn Astronomical Institute; zhou@astro.rug.nl

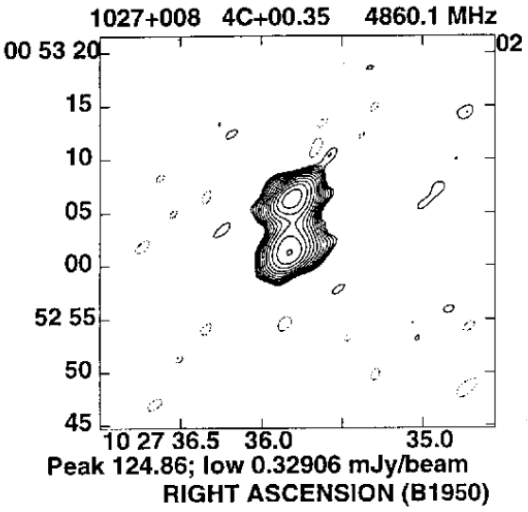

FIG. 2. Ra/Dec map of 4C 00.35, with contour[6].

The angular resolution can vary between 0.2 and 0.04 arcsec, and the observing frequency is between 50 GHz and 73 MHz[4]. The target source in this paper – 4C +00.35, was observed under a VLA B-configuration, at a wavelength of 6cm.

D. 4C +00.35

4C +00.35 is a famous radio galaxy located at $l = 245.3970°, b = 46.7483°$ (Ra =10:27:35.8, Dec = +00.53.03.3, B1950), with angular size $\theta = 5.0''$ and z = 0.746, and flux density $F_\nu = (418 \pm 24)$ mJy[5]. Fig.2 shows an Ra/Dec map of the target of this paper, 4C +00.35, one of the sources from the 4C survey (Pilkington & Scott 1965; Gower et al. 1967). The 4C survey has a limiting flux density of 2 Jy at 178 MHz, consisting most of radio galaxies and quasars. The contour of flux density is also depicted in the figure, and the peak flux density was found to be 124.86 mJy (N. Jackson et al. 1998).

II. OBSERVATION

The observation was performed under a VLA B-configuration[6](see Fig.3) over a frequency peaked at 4860.1 MHz, on Jul 30, 1994. Data were taken in two contiguous bands of 50 MHz bandwidth centered at 4835 MHz and 4885 MHz, respectively. Exposure times were 2 minutes, resulting in a theoretical rms noise level of 0.10 mJy/beam. The observation was done over a total time lapse of 7170s, during which 3 radio galaxies 3C 048, 4C +00.30, and 4C +00.35 (target galaxy) were observed successively. The third observation source is the target of this paper, which was observed from 17:35:50.0 to 17:39:00.0. Table 1 listed the observational parameters

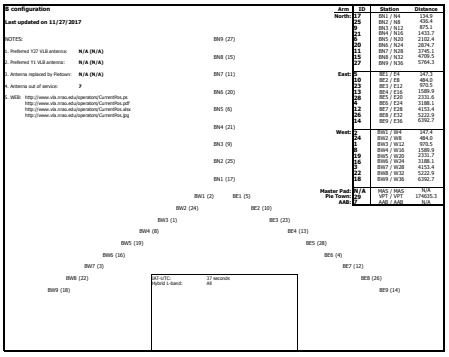

FIG. 3. VLA B-configuration of the 27 antennae[7].

of the sources: where 3C 048 was used as an amplitude

TABLE I. Observational parameters

Object	field	IAU name	Channel(GHz)
3C 048	0	0134+329	4.84
4C +00.30	1	0940+001	4.89
4C +00.35	2	1027+008	both

calibrator, and 4C 00.30 a phase calibrator.

A. Two-element interferometer

The VLA is comprised of 27 antennae, each two of which are identical and perform like a two-element interferometer, which measures the interference pattern produced by two apertures. The response of a interferometer is measured by visibility, which is just the Fourier transform of the sky brightness over a small field of view. Thus, to determine the visibility accurately, amplitude and phase must be calibrated. The quality of visibility can be first inspected by looking at the uv-coverage (shown in Fig.4). The limitations are that when data falls beyond the maximum of u and v, it becomes unresolved; and when it falls within the range of the minimum of u and v, the source is just too large to be detected. Undetected or corrupted source in the image plane would appear as noise in the uv-plane.

B. Calibration procedure

The data reduction and image processing was done using CASA, the Common Astronomy Software Applications package. It is being developed in support of the data post-processing needs of the next generation of radio astronomical telescopes such as ALMA and VLA[8].

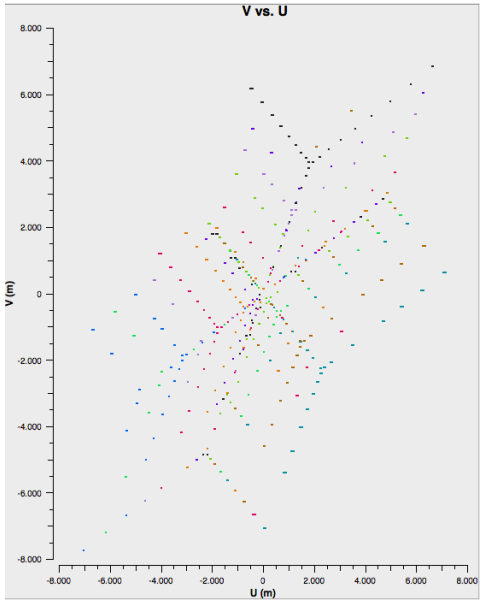

FIG. 4. UV-coverage of 4C +00.35. These tracks are formed by the 2-D projection of the various interferometer baselines on a plane (the so-called "uv-plane") which is perpendicular to the source direction.

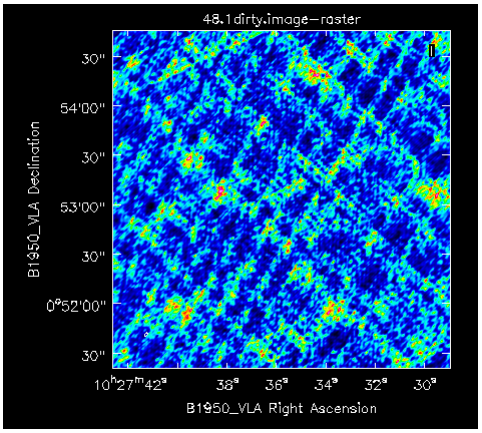

FIG. 5. Dirty image of 4C +00.35, which is just the convolution of the image obtained with the dirty beam (the inverse Fourier of the finite sampling of the uv-plane).

1. *Deriving calibration tables*

The calibration procedure involves phase calibration and amplitude calibration. Flux densities were bootstrapped to the source 3C 048(field 0), using the value of 5.4 Jy at 4850 MHz from Baars et al. (1979). Phase calibration was performed using point source calibrators (here 3C 286) from the VLA Calibrator List (Perley 1982). After which a "dirty image" can be made, without the gain calibrated. Fig.5 shows the so-called dirty image of 4C +00.35.

Having obtained an overall flux scaling, we are at the stage of determining the full gain solutions. This was done by using "*gaincal*", which solves for phase and amplitude response of each telescope as a function of time. A temporal calibration table was made during this procedure. After which we have to apply the absolute flux scaling to calibration table from known source, using *fluxscale*.

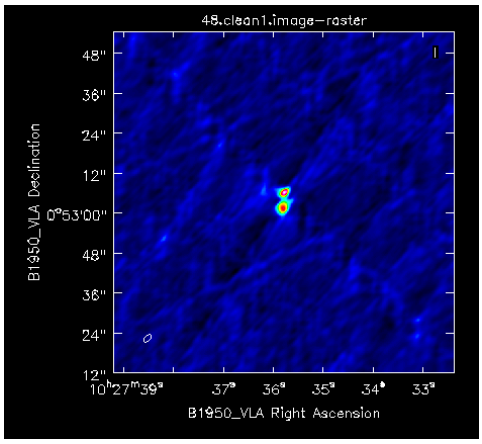

FIG. 6. First cleaned image of 4C +00.35.

2. *Cleaning image*

After applying the calibration tale from previous steps, the first cleaned image (see Fig. 6) was made. Subsequently we need to do self-calibration to phase and amplitude using the CLEAN algorithm. The main idea was to build up flux in the succeedingly fainter part of the image, and create a model image containing a fraction of those flux points. By subtracting the model from the image, a final residual (which contains no suspicious bright points) image was left out. Fig. 7 shows the residual image, where the two square boxes depict the models subtracted. This leads to the final cleaned image (as shown in Fig. 8).

III. RESULTS

A. Flux density and angular size

After getting the final leaned image, the peaked and extended fluxes can be roughly determined. Total flux density was found to be 363.65 mJy and the peaked fluxes were 112.3 and 79.9 mJy (shaped as two coloured ellipses in Fig.7), respectively, with an uncertainty of 27.0 mJy. This was in good agreement with what found in previous literature (total flux density of 377.2 mJy and peaked flux density of 124.9 mJy and 80.1 mJy, respectively, (N. Jackson et al., 1998); total flux density of 404 ± 56, P. C. Gregory et al.). However, these results may not be fully reliable in cases where the components (as depicted in the coloured ellipses) are not well resolved from each

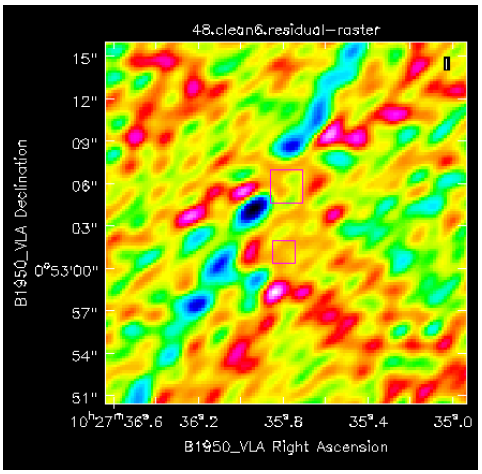

FIG. 7. Residual image of 4C +00.35.

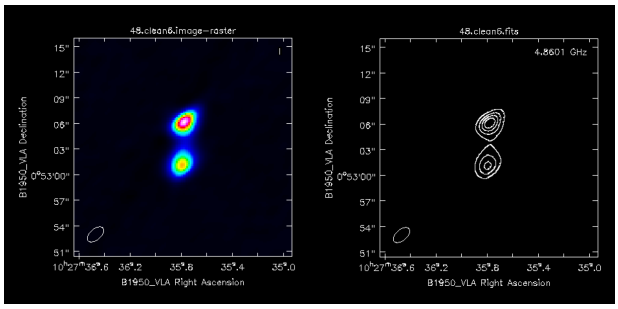

FIG. 8. Final cleaned image of 4C +00.35: one the left panel is the cleaned image in colour and on the right is the contour image (see Fig.2 as reference).

other, or in cases when the components are too large and extended (as in the above-mentioned section). The angular size of 4C +00.35 can also be inferred from the final cleaned image, to be $(5.0 \pm 0.2)''$, which was in good agreement with $4.9''$ (N. Jackson et al., 1998). The uncertainty comes mostly from the resolution limit.

B. Point source sensitivity

Sensitivity gives us information about the performance of a measuring device, and determines the quality of a measurement. The theoretical expected thermal noise of VLA is given by:

$$\sigma_{S_\nu} = \frac{SEFD}{\eta_c \sqrt{n_{pol} N(N-1) t_{int} \Delta\nu}} \qquad (1)$$

where SEFD is the system equivalent flux density (Jy), and for the VLA's 25meter paraboloids, the SEFD is given by the equation $SEFD = 5.62 T_{sys}/_A$, and $_A$ is the antenna aperture efficiency in the given band. $_c$ is the correlator efficiency ($\sim$0.93 with the use of the 8-bit samplers)[9]. t_{int} is the total integration time on source, and here in this observation is 190 s.

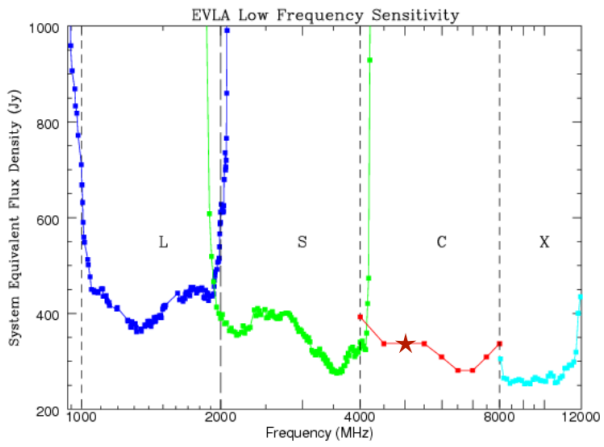

FIG. 9. SEFD profile of VLA, the SEFD of VLA at 5 GHz is 265 Jy (denoted by a star), as can be read from the plot[9].

Thus plugging in $\Delta\nu = 2 \times 50$MHz (because of 2 channels for field 2, see Table 1) and N = 27(number of antennae used in B-configuration in this observation), yields a thermal noise of $\sigma_{5GHz} = 51\mu$Jy. The true deviation of flux density in the background was found to be 248μJy, which was a factor of 4.9 larger than the theoretical value. This may be due to the fact that the image was not totally cleaned (the residual can not be cleaned further), and that there might be large scale sources which are beyond the limit of resolution.

C. Redshift

For 4C +00.35, the redshift z and radial velocity could not be found in the published catalogs, thus the true emission wavelength could not be estimated. A plausible result could not be reached to its redshift and velocity. Further observations are required to infer these two properties.

D. Spectrum profile

The spectral energy distribution for 4C +00.35 can be found in Fig.10[11]. A total number of 33 data points were plotted, as $F_\nu(Jy)$ vs. $\nu(Hz)$. By using a Python package *curvefit*, the spectral index at low frequency range ($\sim (0.738 - 50)10^9 Hz$) and high frequency range ($\sim (3.25 - 8.36)10^{14}$Hz) were found to be -0.69 and -3.74, respectively see the Spectral Energy Distribution (SED) shown in Fig.11. The spectral energy distribution of syn-

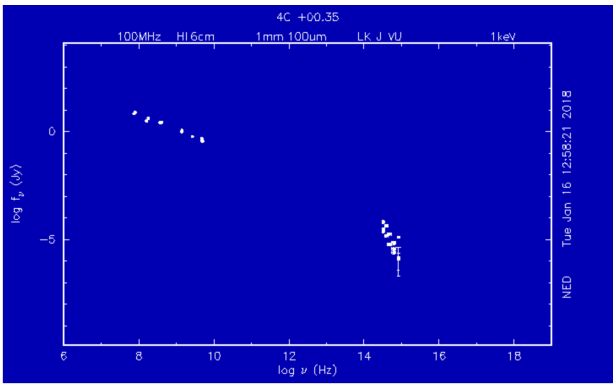

FIG. 10. Spectrum profile of 4C +00.35, 33 data points were plotted, at frequency range $\sim (3.25 - 8.36)10^{14}$Hz, and $\sim (0.738 - 50)10^{9}Hz$[11].

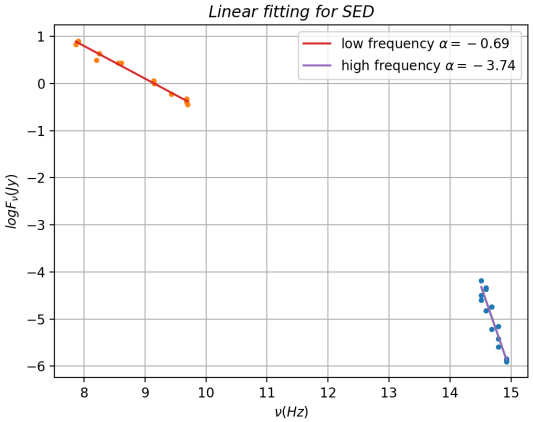

FIG. 11. The fitting for the spectral energy distribution of 4C +00.35, 33 data points were plotted, and the spectral indices were found to be -0.69 and -3.74 for low frequency and high frequency, respectively.

chrotron emission is given by:

$$F_\nu \propto \nu^\alpha \tag{2}$$

where α is the spectral index[10].

IV. DISCUSSION

Table 2 lists all the above-mentioned properties found for 4C +00.35:

The found properties of 4C +00.35 confirm the results presented in N. Jackson et al., 1998. The radial velocity and emission wavelength could not be inferred due to lack of redshift value in the published redshift catalog. The spectral index found for low frequency is ∼-0.69, implying that there is synchrotron radiation going on around this radio galaxy, and that 4C +00.35 is indeed a radio-loud AGN. An educated guess could be that this high energy emission is powered by a super-massive black hole lying

TABLE II. Properties of 4C +00.35

Properties	Values
Ra(B1950)	156.8991542°
Dec(B1950)	0.8844361°
angular size (")	$(5.0 \pm 0.2)''$
total flux density(mJy)	363.65±27.0
peak flux density(mJy)	112.3±27.0
	79.9±27.0
SEFD(Jy)	265
theoretical noise (μJy)	51
found noise (μJy)	248
spectral index(low)	-0.69
spectral index(high)	-3.74

in the central region, and that there might be active star forming regions around 4C +00.35. The steepening at higher frequency range implies that there are high energy electrons radiating away their energy. More measurements are needed in the middle frequency range, to give a logical inferring of the critical point, which provides information about the age and evolution of the galaxy.

V. CONCLUSIONS

In this paper, the properties of a radio-loud galaxy 4C +00.35 were studied, based on the measurements made on Jul 30, 1994. The total flux density and peak flux densities were found, based on the cleaned image obtained, to be 363.65 mJy, and peak densities 112.3 mJy and 79.9 mJy respectively, each having an uncertainty of 27 mJy. The found flux properties are in good agreement with previous literature. Based on the configuration of this observation, a theoretical noise can be deduced, to be 51 μJy, this is a factor of 4.9 smaller than the real noise, which was found to be 248 μJy. This may be due to the fact that the image was not thoroughly cleaned and the residual image still contains suspicious sources. The spectral indices can also be found, based on all the data points listed in the NED database[11]. The spectral index in the lower frequency range was -0.69, which was most likely to be from synchrotron radiation; whereas the spectral index found in the higher frequency range was -3.74, a sharp steepening compared to the lower frequency slope which is most likely to be from old high energy electrons. More data are needed from velocity survey and redshift survey, to make a thorough judgment about the redshift value and radial velocity, in order to infer the age of the galaxy and study the formation and evolution going on around the source.

VI. REFERENCES

[1] X-ray Astronomy
https://www-xray.ast.cam.ac.uk/xray_introduction/AGN_intro.html

[2] The Luminosity of AGNs
http://www.open.edu/openlearn/science-maths-technology/science/physics-and-astronomy/introduction-active-galaxies/content-section-4.3

[3] Super-Massive Black Hole
http://www.science20.com/news/gas_shrouded_activty_galaxy_revealed

[4] VLA
http://www.vla.nrao.edu

[5] The Parkes-MIT-NRAO (PMN) Surveys. VI. Source Catalog for The Equatorial Survey (-9°.5 < δ < +10°.0)
http://articles.adsabs.harvard.edu/cgi-bin/nph-iarticle_query?1995ApJS...97..347G&data_type=PDF_HIGH&whole_paper=YES&type=PRINTER&filetype=.pdf

[6] VLA observations of a 4C equatorial sample. II.
https://aas.aanda.org/articles/aas/pdf/1999/03/ds1513.pdf

[7] VLA-B
http://www.vla.nrao.edu/operators/CurrentPos.pdf

[8] CASA
https://casa.nrao.edu

[9] Sensitivity
https://science.nrao.edu/facilities/vla/docs/manuals/oss/performance/sensitivity

[10] Synchrotron Emission
http://www.astro.caltech.edu/~mmanders/ay121/notes/Lecture_Slides_20131025_Gregg.pdf

[11] Spectral Energy Distribution
https://ned.ipac.caltech.edu/cgi-bin/datasearch?search_type=Photo_id&objid=68108&objname=4C%20%2B00.35&img_stamp=YES&hconst=73.0&omegam=0.27&omegav=0.73&corr_z=1&of=table